

Green synthesis of reduced graphene oxide using *Indigofera tinctoria* leaf extract and its antibacterial activity against *Escherichia coli*

M. Yasser^{1,2} , Abd. Wahid Wahab², Abdul Karim^{2*}, St. Fauziah²

¹ Department of Chemical Engineering, Politeknik Negeri Ujung Pandang, Makassar 90245, South Sulawesi, Indonesia

² Department of Chemistry, Hasanuddin University, Makassar 90245, South Sulawesi, Indonesia

* Corresponding author's e-mail: karimkimia@yahoo.com

ABSTRACT

This article describes a green and sustainable approach for the synthesis of reduced graphene oxide (rGO) using *Indigofera tinctoria* leaf extract as a natural reducing agent. The biogenic IT-rGO was characterized using UV-Vis spectroscopy, FTIR, XRD, and SEM to confirm its successful reduction and to determine its structural properties. The phytochemicals present in the extract, including flavonoids, polyphenols and alkaloids, played a crucial role in reducing GO to rGO. The synthesized rGO exhibited significant antibacterial activity against *Escherichia coli*, with the highest antibacterial activity observed at a 100% IT-rGO concentration, resulting in an inhibition zone value of 10.25 mm against the *E. coli* bacteria. The antibacterial mechanism is proposed to involve membrane disruption and the induction of oxidative stress. The use of *Indigofera tinctoria* not only offers an eco-friendly and cost-effective route for rGO production but also imparts enhanced bioactivity, making the material a promising candidate for biomedical and environmental antibacterial applications.

Keywords: reduced graphene oxide (rGO), green synthesis, *Indigofera tinctoria*, antibacterial, *Escherichia coli*.

INTRODUCTION

The aquatic environment is something that must be preserved. Pollution of water bodies can cause several problems, including the onset of diseases caused by pathogenic microorganisms. *Escherichia coli* (*E. coli*) is a Gram-negative bacterium whose presence in water can cause health problems, such as diarrhoea or digestive tract infections (Abavisani et al., 2023). Along with the increasing resistance of bacteria to antibiotics, the development of effective antibacterial alternatives has become increasingly urgent. Carbon-based nanomaterials, notably reduced graphene oxide (rGO), have attracted attention as potential antibacterial agents (Mann et al., 2021).

Reduced graphene oxide (rGO) is a carbon-based material derived from graphene, exhibiting graphene-like characteristics in terms of its mechanical, optical, and electrical properties. rGO is

produced by removing some oxygen groups from graphene oxide (GO) through the production process and retaining some COOH functional groups at the edges. Some of the advantages of rGO are its good electrical conductivity properties and its large surface area, which is attributed to the presence of defects and oxidised functional groups. rGO has been widely used in various fields, such as sensors (Karim et al., 2024), supercapacitors (Panicker and Sahu, 2021), adsorbents (Wijaya et al., 2020), photocatalysis (Parthipan et al., 2021), and antibacterial (Rakkimuthu et al., 2022). Oxygen functional groups on rGO can interact with bacterial cell membranes, as well as their high conductivity properties, which can induce oxidative stress in microorganisms (Agarwal and Zetterlund, 2021).

A widely used approach in the synthesis of rGO is chemical reduction. The problem is that all the chemicals used, including hydrazine, sodium

borohydride, sodium citrate and hydroquinone, are potentially toxic to human health and pollute the environment (Hu and Gao, 2023). It is essential to develop an environmentally safe method for producing reduced graphene oxide using natural materials, such as microbes and plants.

Green synthesis offers an eco-friendly alternative by utilising natural products as reducing agents. Plant extracts, in particular, have proven to be effective in reducing GO due to the presence of bioactive compounds. These compounds not only facilitate the reduction of GO but also stabilise the resulting rGO through surface functionalisation (Singh et al., 2023). This approach aligns with the principles of green chemistry, emphasising the use of renewable resources and minimising environmental impacts. Biomolecules from the polyphenol group and other secondary metabolites in plants serve as reducing agents in the synthesis of rGO (Kurian, 2021).

Among the various plants explored for green synthesis, *Indigofera tinctoria*, a member of the Fabaceae family, stands out due to its rich phytochemical composition. Traditionally used as a source of natural indigo dye, *Indigofera tinctoria* includes several bioactive molecules, namely alkaloids, flavonoids, and tannins, which possess substantial reducing and capping capabilities (J.O, 2021; Wahyuningsih et al., 2017). These properties make it an ideal candidate for reducing GO under environmentally benign conditions. The identified *Indigofera tinctoria* leaf extract contains phenolic compounds (Mishra et al., 2020), such as 5-Hydroxy-L-tryptophan (Rajan et al., 2015; Rajab et al., 2025). The reducing ability of *Indigofera tinctoria* leaf extract has been proven by its ability to reduce gold and silver to nanoparticle size (Vijayan et al., 2018).

The importance of applying green solutions to solve environmental problems, such as environmental pollution caused by bacteria, highlights the need to utilise rGO synthesised from *Indigofera tinctoria* leaf extract as a solution for environmentally friendly antibacterial purposes. This research aims to investigate the effectiveness of *Indigofera tinctoria* extract in reducing GO, characterise the resulting rGO, and evaluate its potential as an antibacterial agent against *E. coli*. By adopting a green synthesis approach in the preparation of rGO, this study contributes to the development of sustainable nanotechnology while reducing the environmental risks associated with conventional chemical reduction

methods. Additionally, it provides a solution for treating diseases caused by *E. coli* bacteria originating from aquatic environments.

MATERIALS AND METHODS

Materials

GO as a precursor in synthesizing rGO was obtained from Nanomaterials for Renewable Energy Research Center (NRE LAB) Indonesia. Fresh leaves of *Indigofera tinctoria* were obtained from Bulukumba Regency, South Sulawesi Province.

Extraction of *Indigofera tinctoria*

The leaves of *Indigofera tinctoria* were initially cleaned, dried, and then ground into a powder. A total of 10 grams of this leaf powder was extracted using 100 mL of distilled water as the solvent, which was then heated to boiling for 30 minutes. Following this, the mixture was filtered to separate the precipitate from the filtrate. The filtrate was collected in a bottle for use as a bioreductor in the synthesis of rGO (Yasser et al., 2021; Yasser et al., 2021; Yasser et al., 2020). The extract was concentrated using a rotary vacuum evaporator. The concentrated extract was then characterized using phytochemical testing, IR spectroscopy, and Gas Chromatography-Mass Spectrometry (Alamsjah et al., 2024 ; Yasser et al., 2020).

Green synthesis of IT-rGO

In this project, we green-synthesised rGO using the aqueous extract of *Indigofera tinctoria* leaves as a reductant. The green synthesis was achieved by reacting GO with an aqueous extract from *Indigofera tinctoria* leaves in a 1:1 (v/v) ratio at 85 °C. A 50 mL GO solution (1 mg/mL) was reacted with 50 mL of an aqueous extract of *Indigofera tinctoria* leaves. The mixture was reacted on a hot plate at a heating temperature of 85 °C and stirred using a magnetic stirrer for 12 hours. After the heating process was complete, the mixture was filtered to separate the precipitate and filtrate. The precipitate was then washed with water and ethanol until the pH of the precipitate reached 7. The precipitate was then oven-dried at 60 °C for 12 hours (Wijaya et al., 2020).

UV-Vis spectroscopy characterization

The IT-rGO solid formed from the green synthesis process was dissolved in aqueous solvent. UV-Vis spectroscopy was employed to characterize the IT-rGO solution at wavelengths between 200 to 700 nm.

Fourier transform infrared spectroscopy (FTIR) characterization

The IT-rGO material was mixed with KBr crystals until a homogeneous mixture was obtained. The homogeneous mixture was characterized with IR Prestige-21 Shimadzu at a measurement range of 4000–500 cm^{-1} .

X-ray diffraction (XRD) characterization

The crystal confirmation was determined using a Bruker D8 Advance X-Ray diffractometer (XRD) at a measurement range between 5° – $89,990^\circ$, a scan speed of 0.10 deg/min and at room temperature (25°C).

Scanning electron microscope-energy dispersive X-ray characterization

The morphology of IT-rGO was examined utilizing SEM, Hitachi SU3500, accelerating voltage 10kV and maximum magnification 100 k. The elemental composition was examined using EDAX TEAM.

Escherichia coli antibacterial activity

Sensitivity testing is done to assess the effectiveness of antibiotic use. This antibiogram uses the Kirby-Bauer method by taking colonies of each test bacterium *Escehrichia coli* ATCC 25923 which were grown for 24 hours previously and suspended in 1 ml of 0.9% NaCl to reach turbidity (Sabee et al., 2020). Then using a sterile swab, the bacterial suspension was applied (swab) evenly on Muller Hinton Agar (MHA) media and placed paper disks that previously contained IT-rGO with various concentrations, concentrations of 100% (100 mg/100 μL), 50% (50 mg/100 μL), 25% (25 mg/100 μL), 12.5% (12.5 mg/100 μL), 6.25% (6.25 mg/100 μL), 3.125% (3.125 mg/100 μL), on the media and incubated for 24 hours (10). Positive control used chloramphenicol antibiotic 30 μg /disk and negative control used distilled

water. Observations were made on the disc paper to measure the diameter of the inhibition zone, the value of the inhibition zone produced indicates the level of the IT-rGO ability as an anti-bacterial against the test bacteria *Escehrichia coli* ATCC 25923.

RESULTS AND DISCUSSION

Characterization of extract

The secondary metabolite compounds of each plant depend on several factors, including differences in the growth environment and the polarity of the solvents. The qualitative identification of secondary metabolites is characterised by physical changes, such as colour changes and the formation of specific precipitates when the sample is reacted with a specialised reagent (Mulia et al., 2023). Phytochemical tests on the aqueous extract of *Indigofera tinctoria* yielded positive results for the presence of secondary metabolite compounds, including alkaloids, flavonoids, and phenolics (Table 1). These results demonstrate differences in the outcomes of phytochemical testing using various solvents and regions, specifically in the case of *Inigofera tinctoria* plants growing. Venkatachalam (2018) demonstrated that the aqueous extract of *Indigofera tinctoria* leaves contained secondary metabolite compounds, including flavonoids, phenolics, and terpenoids. The difference in the results obtained for alkaloids and terpenoids shows that differences in plant growing locations affect the content of secondary metabolites (Venkatachalam, 2018).

The phytochemical analysis of *Indigofera tinctoria* leaf extract was strengthened by the results of measuring the extract using IR spectroscopy to determine the functional groups in the extract (Figure 1 and Table 2). The extract was identified as containing an aromatic ring

Table 1. Phytochemical test results of *Indigofera tinctoria* leaf extract

| Metabolite compounds | Test result |
|----------------------|-------------|
| Alkaloid | + |
| Flavonoid | + |
| Polyphenols | + |
| Triterpenoid | - |
| Steroid | - |

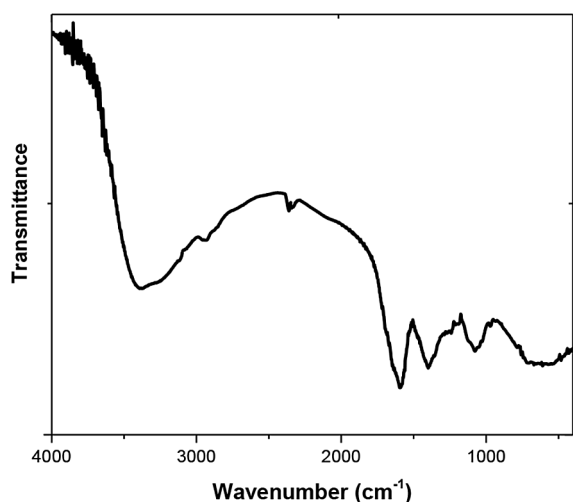


Figure 1. FTIR spectrum of *Indigofera tinctoria* leaf extract

Table 2. Possible functional group of *Indigofera tinctoria* leaf extract

| Wavenumber (cm ⁻¹) | Possible functional group |
|--------------------------------|---|
| 3394.83 | Hydroxyl (-OH) |
| 1591.33 | Aromatic ring (C=C-C) |
| 1400.37 | Phenol or tertiary alcohol |
| 1076.32 | C-O bonds or primary amines (-CN stretch) |
| 711.76 | C-H bond (ortho aromatic) |

(C=C-C) characterized by the presence of absorption at wave numbers around around 1591.33cm⁻¹ (Coates, 2000). The presence of this aromatic ring is confirmed by the absorption at wave number 711.76 cm⁻¹, which is a C-H bond (ortho aromatic). Hydroxyl (-OH) groups were identified at 3394.83 cm⁻¹ and 1400.37 cm⁻¹ as phenol or tertiary alcohol. The IR spectrum also found an absorption at 1076.32 cm⁻¹ which allows the presence of C-O bonds (alcohols, ethers or glycoside groups) or the presence of primary amines (-CN stretch) (Nandiyanto et al., 2019). The results of characterization by IR spectroscopy of *Indigofera tinctoria* leaf extracts are in consistence with the results of its phytochemical test. The presence of flavonoid and phenolic secondary metabolite compounds is characterized by the identification of aromatic rings, hydroxyl groups (-OH) and phenol groups. While the presence of alkaloids is confirmed by the presence of primary amine (-CN) contained in the extract. The presence of nitrogen atoms (N) is a factor that indicates the presence of Alkaloid group compounds.

The chromatogram (Figure 2) of *Indigofera tinctoria* leaf extract was identified as containing 59 compounds (Table 3), some of which consisted of polyphenol, flavonoid (Phenanthrenol) and alkaloid (Quinoline) compounds. The presence of the three types of compounds confirmed the results of phytochemical tests and IR spectroscopy, which also found the presence of these compounds in the extract.

Characterization of rGO

The UV-Vis spectrum (Figure 3) of GO shows maximum absorption at a wavelength of 230.64 nm, which means π - π^* transition of aromatic C=C bond interaction (Tahir et al., 2023; Mombeshora and Muchuweni, 2023) and a shoulder peak at ~300 nm due to n- π^* transition of carbonyl group (Jin et al., 2018 ; Lingaraju et al., 2019). The UV-Vis spectrum of IT-rGO synthesized using *Indigofera tinctoria* leaf extract has a maximum absorption at a wavelength of 270 nm. This shows that there has been a red shift from a wavelength of 230 nm to a wavelength of 270 nm, which means that there has been a π - π^* transition from the C = C aromatic bond. The removal of oxygen groups has occurred through reduction with *Indigofera tinctoria* leaf extract (Perumal et al., 2022; Ghosh et al., 2021).

The functional group of GO and IT-rGO was examined within 4000–500 cm⁻¹ (Figure 4 and Table 4). FTIR spectrum of GO shows the presence of functional groups such as hydroxyl groups (-OH) with a broad peak at 3444.02 cm⁻¹, the presence of a peak at 1703.29 cm⁻¹ indicating

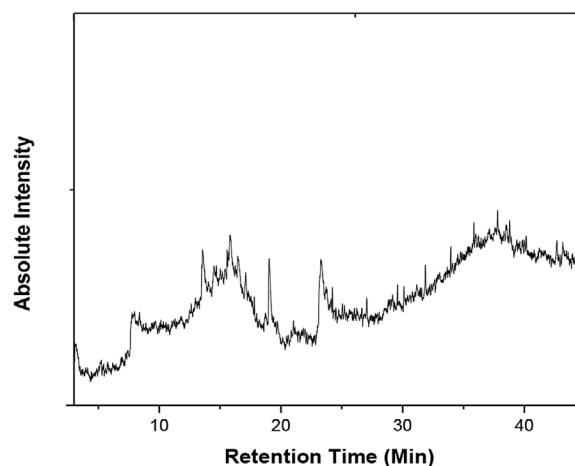


Figure 2. Chromatogram of *Indigofera tinctoria* L. leaf extract

Table 3. Chemical composition of *I. tinctoria* L. leaf extract

| No. | RT (min) | Compounds name | No. | RT (min) | Compounds name |
|-----|----------|--|-----|----------|--|
| 1 | 7.258 | 2,4-Octadienoic acid, 7-(t-butyltrimethylsilyloxy)-, methyl ester (E,E)- | 31 | 24.387 | Heptadecyl acetate |
| 2 | 7.375 | 7-(N,N-Diallylamino)-2-methyl-5-heptyn-3-ol | 32 | 24.510 | 1,2-Oxathiane, 6-dodecyl-, 2,2-dioxide |
| 3 | 7.683 | 1-BUTANOL, 3-METHYL-, ACETATE | 33 | 25.050 | 18-Nonadecenoic acid |
| 4 | 8.382 | 2-Penten-1-ol, (Z)-, TMS derivative | 34 | 26.038 | Cyclotetradecane |
| 5 | 13.333 | Quinoline-5,8-dione-6-ol, 7-[[[4-(cyclohexylbutyl)amino]methyl]- | 35 | 26.637 | Octyl palmitoleate |
| 6 | 13.500 | 3,6,9,12-Tetraoxatetradecan-1-ol | 36 | 26.783 | 3.ALPHA.,20.ALPHA.-BIS-TERT-BUTYLDIMETHYLSILYL-ETHER |
| 7 | 13.567 | 5-Aminosalicilic acid, N,O,O'-tris(trimethylsilyl)- | 37 | 27.045 | Amodiaquine, 2TMS derivative |
| 8 | 13.733 | 1-Bromo-1-methyl-1-silacyclohexane | 38 | 27.766 | 1H-phosphindole, 2,3-dihydro-1,3,3,4,6-pentamethyl-, 1-oxide |
| 9 | 13.875 | p-Mentha-6,8-dien-2-one, semicarbazone | 39 | 28.808 | 1,5-Naphthalenedione, octahydro-4a-methyl- |
| 10 | 14.042 | ETHANE, 1,1'-OXYBIS[2-ETHOXY- | 40 | 29.169 | Bicyclopropyl derivative |
| 11 | 14.483 | Oleyl alcohol, trifluoroacetate | 41 | 29.580 | 1H-Purin-6-amine, [(2-fluorophenyl)methyl]- |
| 12 | 14.695 | Octadecane (CAS) | 42 | 30.109 | trans-2-Hexadecenoic acid |
| 13 | 15.015 | 3,7,11-Trimethyldodecylacetate | 43 | 31.565 | 2,3 Dinor thromboxane b2 tetra-TMS |
| 14 | 15.392 | 1-Heptatriacotanol | 44 | 31.861 | Silicone oil |
| 15 | 15.576 | 5-Bromo-3-ethyl-3-hydroxyindolin-2-one, 2TBDMS derivative | 45 | 33.956 | Cyclodecasiloxane, eicosamethyl- |
| 16 | 15.650 | MOME INOSITOL | 46 | 35.533 | Dihydroindolizine derivative |
| 17 | 15.806 | Tetradecanoic acid (CAS) | 47 | 35.700 | Trimethylbenzimidazole derivative |
| 18 | 16.217 | 1,3,6-Trioxa-2-silacyclooctane, 2,2,-dimethylsilyl- | 48 | 35.848 | Biphenylenecarboxylic acid derivative |
| 19 | 16.461 | PLUCHIDIOL | 49 | 35.975 | Spiro dioxaspiro derivative |
| 20 | 17.108 | 3,6,9,12-Tetraoxatetradecan-1-ol | 50 | 36.21 | Silicone oil |
| 21 | 17.817 | EICOSAMETHYLCYCLODECASILOXANE | 51 | 36.449 | Isopropyl .gamma.-(p-nitrophenyl)-.alpha.-methylene-.beta.-hydropropanoate |
| 22 | 19.029 | n-Hexadecanoic acid | 52 | 37.806 | Silicone Oil |
| 23 | 21.031 | Benzoic acid, 4-amino-2-hydroxy-, tris(trimethylsilyl) deriv. | 53 | 38.490 | 9.beta.-Acetoxy-3,5.alpha.,8-trimethyltricyclo[6.3.1.0(1,5)]dodec-3-ene |
| 24 | 22.130 | 1,2-Epoxy nonane | 54 | 38.782 | 3-PHENANTHRENOL, 4B,5,6,7,8,8A,9,10-OCTAHYDRO-4B,8,8-TRIMETHYL-, (4 |
| 25 | 22.883 | (E)-4-Chloro-2,3-dimethyl-1,3-hexadiene | 55 | 40.003 | Acetamide, N-[[2-(1,1-dimethylethyl)-6-oxo-1,3-dioxan-4-yl]methyl]-, (2R-cis)- |
| 26 | 23.183 | Oleic Acid | 56 | 40.145 | Silikonfett |
| 27 | 23.275 | 9-Octadecenoic acid, (E)- | 57 | 42.114 | Heptasiloxane, hexadecamethyl- (CAS) |
| 28 | 23.508 | 2,3,6-Trimethylhept-6-en-1-ol | 58 | 42.677 | 2-[3-(AMINOMETHYL)-5,7-DIMETHYL-1-ADAMANTYL]ETHANAMINE |
| 29 | 23.718 | Octadecanoic acid | 59 | 43.964 | Tetrasiloxane, decamethyl- (CAS) |
| 30 | 24.226 | 5-Bromo-3-ethyl-3-hydroxyindolin-2-one, 2TBDMS derivative | | | |

the presence of C=O bonds, the presence of epoxy groups at a peak of 1221.44 cm⁻¹, the C-O stretch of C-OH at a peak of 1037.44 cm⁻¹; and the bond between C=C at a peak of 1642.39 cm⁻¹ indicating the basic framework of graphene in the form of aromatic carbon (Parthipan et al., 2021). FTIR spectrum of IT-rGO, it appears that the typical

peak of the C=O functional group (1703.29 cm⁻¹) has not been detected in the FTIR spectrum, the intensity of the typical peak of the epoxy group and the C-O stretch of C-OH decreased in intensity as the synthesis time is lengthened (Shahane and Sidhaye, 2018). This shows that the reduction process has been successfully carried out with the

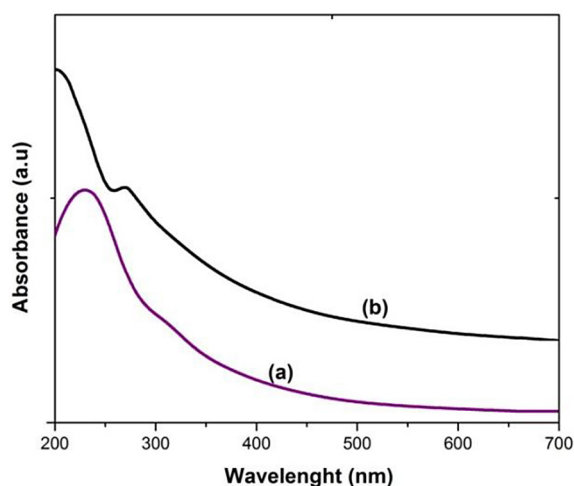


Figure 3. UV-Vis spectrum of GO (a) and IT-rGO (b)

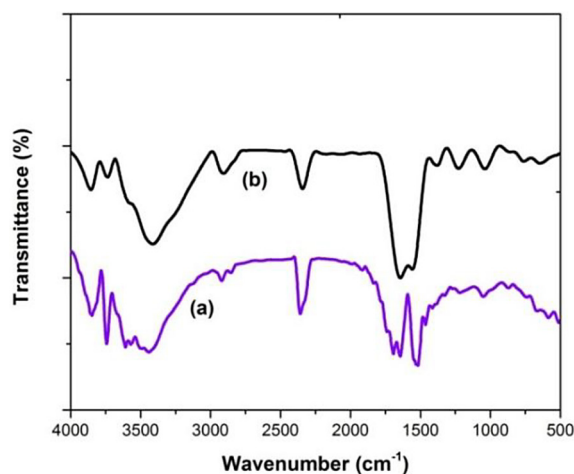


Figure 4. FTIR spectrum of GO (a) and IT-rGO (b)

removal of several oxygen groups (Parthipan, Cheng, et al., 2021).

The XRD patterns produced on GO and IT-rGO show their distinctive peaks (Figure 5). The GO diffraction peak appears at 9.362° , while the IT-rGO synthesized with *Indigofera tinctoria* leaf extract has a broad diffraction peak of about 23.885° . The peak shift from 9.362° to 23.885°

indicates that a reduction process has occurred by reducing the number of oxygen functional groups present in GO (C. Agarwal et al., 2019 ; Faiz et al., 2020). It also indicates that the conjugated graphene network of sp^2 hybrid carbon has been restored during the reduction process (Shubha et al., 2017 ; Nawaz et al., 2017; Rai et al., 2020).

The morphological characteristics of GO and IT-rGO samples were examined using SEM imaging (Figure 6). The GO samples exhibit smooth, wrinkled, and folded surfaces. The presence of wrinkles and folds on the GO surface is attributed to the abundance of functional groups, such as epoxy, hydroxyl, and carboxyl, attached to it (Mahendran et al., 2020 ; Meka Chufa et al., 2021). In contrast, the surface morphology of IT-rGO reveals a reduction in wrinkles, resulting in a structure characterized by folded and overlapping sheets (Kumar, et al., 2022 ; Shubha et al., 2017). This observation indicates the successful reduction of GO using *Indigofera tinctoria* leaf extract.

The Energy Dispersive Spectroscopy (EDS) analysis depicted in Figure 7 demonstrates the composition ratio of carbon (C) and oxygen (O) elements (C/O) before and after the reduction of GO using *Indigofera tinctoria* leaf extract. The presence of numerous epoxy, hydroxyl, and carboxyl groups remains attached to the GO structure, resulting in a C/O ratio of 1.3 (56.51 : 43.49). In contrast, the C/O ratio for the rGO is 3.8 (79.17 : 20.83), indicating the successful reduction of GO through the application of *Indigofera tinctoria* leaf extract. The shift in the C/O atomic ratio from 1.3 to 3.8, as determined by EDS analysis, quantitatively confirms the reduction efficiency. This finding aligns with the changes observed in UV-Vis, FTIR, and XRD analyses, collectively corroborating the restoration of the sp^2 carbon network and the partial removal of oxygen-containing groups.

The GO reduction process that occurs cannot be separated from the presence of polyphenol

Table 4. FTIR spectrum analysis of GO and rGO

| Wavenumber (cm ⁻¹) | | Functional group | References |
|--------------------------------|---------|-------------------------|---|
| GO | IT-rGO | | |
| 3444.02 | 3421.30 | Hydroxyl (-OH) | (Nandiyanto et al., 2019 ; Mahendran et al., 2020) |
| 1703.29 | - | Carbonyl/Carboxyl (C=O) | (Mahiuddin and Ochiai, 2021 ; Sabayan et al., 2020) |
| 1642.39 | 1645.33 | C=C | (Bhattacharya et al., 2017 ; Shubha et al., 2017) |
| 1221.44 | 1226.76 | Epoxy (C-O) | (Yang et al., 2021 ; Punniyakotti et al., 2021) |
| 1053.32 | 1039.66 | C-O stretch of C-OH | (Phukan et al., 2019; Sabayan et al., 2020) |

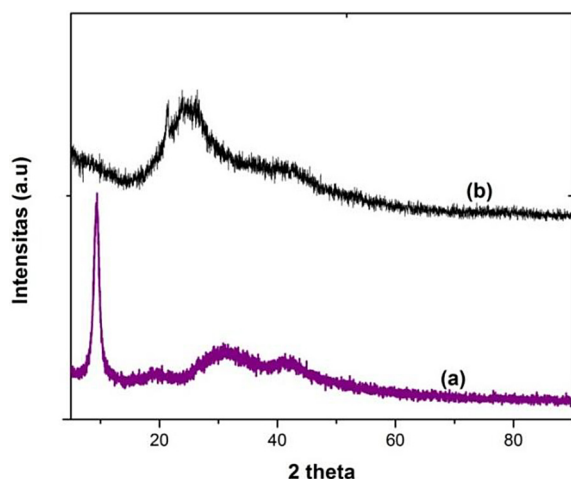


Figure 5. Diffractogram of GO (a) and IT-rGO (b)

groups in the *Indigofera tinctoria* leaf extract. Oxidized polyphenols in the extract can interact with rGO sheets through π - π stack interactions, causing electrostatic repulsion between the rGO layers that triggers stabilization (Qi et al., 2021). aqueous extracts from *Indigofera tinctoria* leaves were found to contain various classes of chemical compounds, including polyphenol,

flavonoids and alkaloid (Venkatachalam, 2018). An illustration of the rGO synthesis mechanism can be seen in Figure 8.

Antibacterial activity of IT-rGO

The antibacterial efficacy of IT-rGO against *E. coli*, a gram-negative bacterium, was assessed. The results, as depicted in Figure 9, demonstrate the extract's inhibitory effect on bacterial growth, evidenced by the inhibition zones observed at various IT-rGO concentrations. Specifically, the inhibition zones for *E. coli* at IT-rGO concentrations of 100%, 50%, 25%, 12.5%, 6.25%, and 3.125% were measured at 10.25 mm, 8.60 mm, 6.70 mm, 4.50 mm, 2.00 mm, and 1.30 mm, respectively (Table 5).

The antibacterial efficacy of IT-rGO against *E. coli* exhibits varying levels of inhibition, classified as strong, moderate, and weak. This variability in bacterial inhibition is attributed to the concentration of materials employed in the antibacterial activity assays. This observation aligns with the findings of Thiyagarajulu et al. (2020), who reported positive inhibition against pathogenic bacteria at

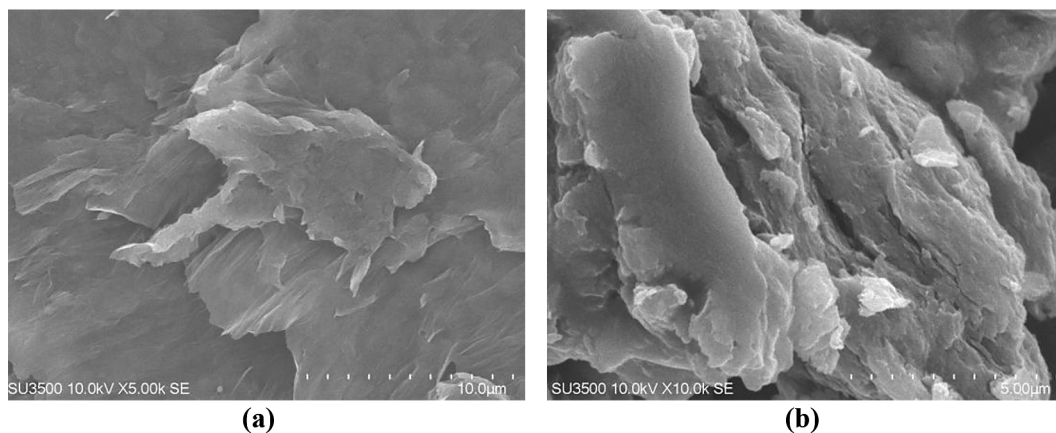


Figure 6. SEM image of GO (a) and IT-rGO (b)

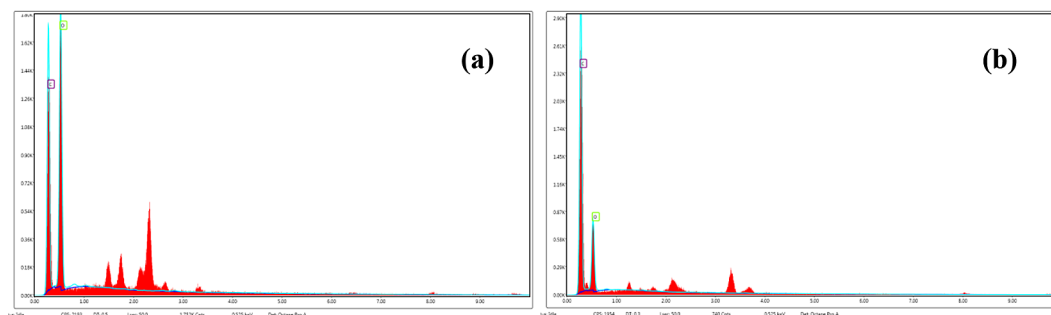


Figure 7. EDS spectra of GO (a) and IT-rGO (b)

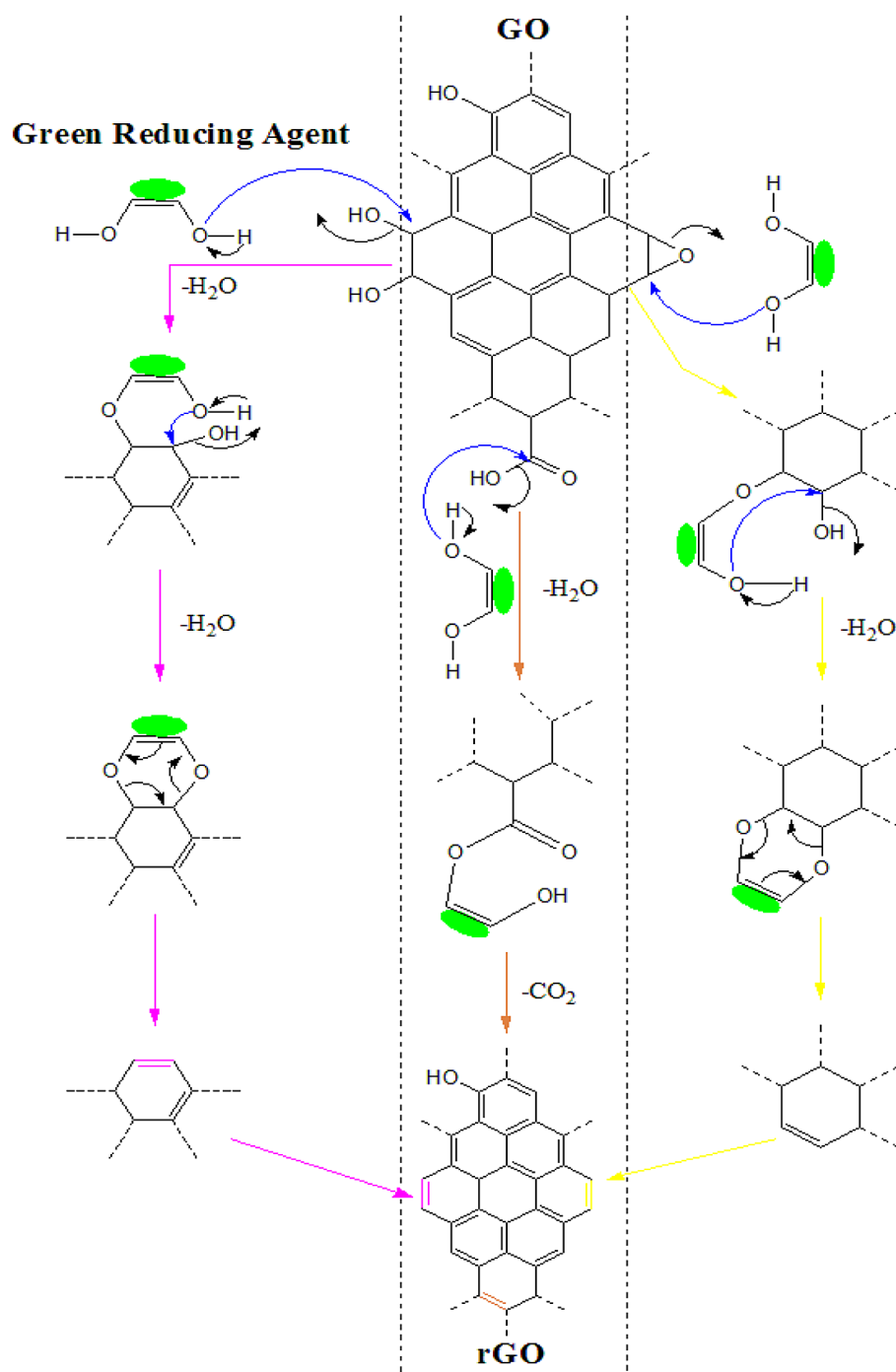


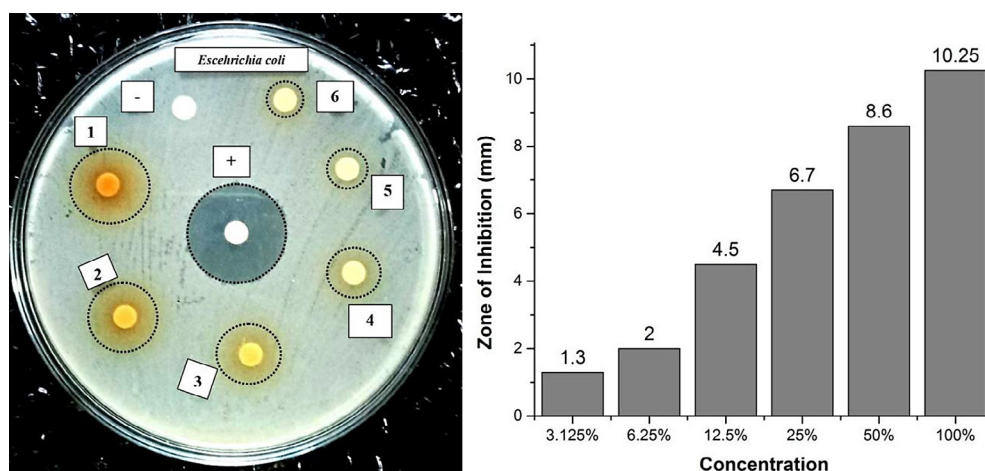
Figure 8. Green synthesis mechanism illustration of rGO

IT-rGO concentrations of 25%, 50%, 75%, and 100%, with inhibition zone values increasing proportionally with higher IT-rGO concentrations (Thiyagarajulu and Arumugam, 2021). The antibacterial activity of IT-rGO demonstrated the highest efficacy against *E. coli* at a 100% IT-rGO concentration. At a 100% concentration, IT-rGO produced an inhibition zone of 10.25 mm, while the standard antibiotic (positive control) exhibited an inhibition zone of 19.50 mm. According to

established criteria for antibacterial efficacy, inhibition zones greater than 10 mm are classified as indicative of strong antibacterial activity. Thus, although IT-rGO exhibited a slightly lower efficacy than conventional antibiotics, its activity remains within a strong category. Beyond this, the practical applicability of IT-rGO is noteworthy. The green synthesis approach eliminates toxic reducing agents, offering an environmentally friendly and cost-effective route to produce rGO.

Table 5. Inhibition zone diameter antimicrobial test of IT-rGO

| Concentrations | Inhibitory zone diameter (mm) | Inhibition category |
|--------------------------------|-------------------------------|---------------------|
| Chloramphenicol (+) 30 µg/disk | 19.50 | Strong |
| 100% | 10.25 | Strong |
| 50% | 8.60 | Medium |
| 25% | 6.70 | Medium |
| 12.5% | 4.50 | Weak |
| 6.25% | 2.00 | Weak |
| 3.125% | 1.30 | Weak |

**Figure 9.** Zone of inhibition against *E. Coli* bacteria by rGO

The antibacterial efficacy of IT-rGO is attributed to the interaction between graphene and microbial cells, which leads to adhesion on the bacterial cell surface, resulting in cell membrane disruption and oxidative stress (Lim et al., 2012). Additionally, the presence of secondary metabolite compounds in *Indigofera tinctoria* leaf extracts, such as alkaloids, phenols, and flavonoids, on the surface of IT-rGO nanosheets further enhances the bactericidal effect (Thiyagarajulu and Arumugam, 2021; Khanam and Hasan, 2019).

CONCLUSIONS

This study successfully demonstrated a green and sustainable route for the synthesis of rGO using *Indigofera tinctoria* leaf extract as a natural reducing agent. The presence of phytochemicals, such as flavonoids, polyphenols and alkaloids, played a significant role in the effective reduction of graphene oxide to rGO. Comprehensive characterization via UV-Vis, FTIR, XRD, and SEM-EDS confirmed the structural and morphological

changes associated with the reduction process. The biosynthesized IT-rGO exhibited antibacterial activity against *Escherichia coli*, as evaluated using the Kirby-Bauer disk diffusion method. The highest antibacterial performance was observed at 100% IT-rGO concentration, with an inhibition zone diameter of 10.25 mm, indicating a strong antibacterial effect. These findings suggest that *Indigofera tinctoria*-mediated rGO holds promising potential as an eco-friendly and effective antibacterial nanomaterial for biomedical and environmental applications. This study highlights the potency of rGO as an environmental-friendly antibacterial agent and functional material for applications in sensors, photocatalysis, and energy.

Acknowledgements

The authors would like to thank the Indonesia Endowment Funds for Education (LPDP) and the Center for Higher Education Funding and Assessment (PPAPT-BPI) Ministry of Higher Education, Science and Technology of Republic Indonesia (Grant Number: 03208/J5.2.3./BPI.06/10/ 2022) for the financial support of this work.

REFERENCES

1. Abavisani, M., Bostanghadiri, N., Ghahramanpour, H., Kodori, M., Akrami, F., Fathizadeh, H., Hashemi, A., Rastegari-Pouyani, M. (2023). Colistin resistance mechanisms in Gram-negative bacteria: a Focus on *Escherichia coli*. *Letters in Applied Microbiology*, 76(2), ovad023.
2. Agarwal, C., Singh, M. N., Sharma, R. K., Sagdeo, A., Csóka, L. (2019). In situ green synthesis and functionalization of reduced graphene oxide on cellulose fibers by cannabis sativa L. extract. *Materials Performance and Characterization*, 8(3). <https://doi.org/10.1520/MPC20180149>
3. Agarwal, V., Zetterlund, P. B. (2021). Strategies for reduction of graphene oxide – A comprehensive review. *Chemical Engineering Journal*, 405(127018), 1–29. <https://doi.org/10.1016/j.cej.2020.127018>
4. Alamsjah, F., Fandini, S., Mildawati, M. (2024). Short communication: Evaluation of antibacterial activities and phytochemical composition of ethanolic extract of *Diplazium esculentum*. *Biodiversitas*, 25(3), 937–941. <https://doi.org/10.13057/biodiv/d250304>
5. Bhattacharya, G., Sas, S., Wadhwa, S., Mathur, A., McLaughlin, J., Roy, S. S. (2017). Aloe vera assisted facile green synthesis of reduced graphene oxide for electrochemical and dye removal applications. *RSC Advances*, 7(43), 26680–26688. <https://doi.org/10.1039/c7ra02828h>
6. Coates, J. (2000). Interpretation of infrared spectra, a practical approach. *Encyclopedia of Analytical Chemistry*, 12, 10815–10837.
7. Mishra, D., Gomare, K.S., Sheelwant, S.V. (2020). GC-MS analysis and phytochemical screening of *Indigofera tinctoria* (Linn.) Leaf extract characterizing its medicinal use. *International Journal of Ayurvedic Medicine*, 11(2), 289–299.
8. Faiz, M. S. A., Azurahaman, C. A. C., Raba, S. A., Ruzniza, M. Z. (2020). Results in physics low cost and green approach in the reduction of graphene oxide (GO) using palm oil leaves extract for potential in industrial applications. *Results in Physics*, 16(102954), 1–7. <https://doi.org/10.1016/j.rinp.2020.102954>
9. Ghosh, S., Das, P., Sen, M. B. (2021). Plant extract assisted synthesis of reduced graphene oxide sheet and the photocatalytic performances on cationic and anionic dyes to decontaminate wastewater. *Advances in Natural Sciences: Nanoscience and Nanotechnology*, 12(15008), 1–8. <https://doi.org/10.1088/2043-6254/abde41>
10. Hu, Y., Gao, H. (2023). Chemical synthesis of reduced graphene oxide: a review. *Minerals and Mineral Materials*, 2(2), 1–14. <https://doi.org/10.20517/mmm.2023.07>
11. J.O, A. (2021). Chemical evaluation of proximate, vitamin and amino acid profile of leaf, stem bark and root of *indigofera tinctoria*. *Biomedical Research and Clinical Reviews*, 3(1), 1–6. <https://doi.org/10.31579/2692-9406/026>
12. Jin, X., Li, N., Weng, X., Li, C., Chen, Z. (2018). Green reduction of graphene oxide using eucalyptus leaf extract and its application to remove dye. *Chemosphere*, 208, 417–424. <https://doi.org/10.1016/j.chemosphere.2018.05.199>
13. Karim, A., Yasser, M., Ahmad, A., Natsir, H., Wahid Wahab, A., Fauziah, S., Taba, P., Pratama, I., Rosalin, R., Rajab, A., Nur Fitriani Abubakar, A., Widayati Putri, T., Munadi, R., Fudhail Majid, A., Nur, A., Fadliah, F., Rifai, A., Syahrir, M. (2024). A review: Progress and trend advantage of dopamine electrochemical sensor. *Journal of Electroanalytical Chemistry*, 959(118157), 1–15. <https://doi.org/10.1016/j.jelechem.2024.118157>
14. Khanam, P. N., Hasan, A. (2019). Biosynthesis and characterization of graphene by using non-toxic reducing agent from *Allium Cepa* extract: Anti-bacterial properties. *International Journal of Biological Macromolecules*, 126, 151–158.
15. Kumar, N., Setshedi, K., Masukume, M., Ray, S. S. (2022). Facile scalable synthesis of graphene oxide and reduced graphene oxide: comparative investigation of different reduction methods. *Carbon Letters*, 32(4), 1031–1046. <https://doi.org/10.1007/s42823-022-00335-9>
16. Kurian, M. (2021). Recent progress in the chemical reduction of graphene oxide by green reductants—A Mini review. *Carbon Trends*, 5(100120), 1–7. <https://doi.org/10.1016/j.cartre.2021.100120>
17. Lim, H. N., Huang, N. M., Loo, C. H. (2012). Facile preparation of graphene-based chitosan films: Enhanced thermal, mechanical and antibacterial properties. *Journal of Non-Crystalline Solids*, 358(3), 525–530.
18. Lingaraju, K., Naika, H. R., Nagaraju, G., Nagabhushana, H. (2019). Biocompatible synthesis of reduced graphene oxide from *Euphorbia heterophylla* (L.) and their in-vitro cytotoxicity against human cancer cell lines. *Biotechnology Reports*, 24(e00376), 1–6. <https://doi.org/10.1016/j.btre.2019.e00376>
19. Mahendran, G. B., Ramalingam, S. J., Rayappan, J. B. B., Kesavan, S., Periathambi, T., Nesakumar, N. (2020). Green preparation of reduced graphene oxide by *Bougainvillea glabra* flower extract and sensing application. *Journal of Materials Science: Materials in Electronics*, 31(17), 14345–14356. <https://doi.org/10.1007/s10854-020-03994-4>
20. Mahiuddin, M., Ochiai, B. (2021). Lemon juice assisted green synthesis of reduced graphene oxide and its application for adsorption of methylene blue.

- Technologies*, 9(96), 1–20. <https://doi.org/10.3390/technologies9040096>
21. Mann, R., Mitsidis, D., Xie, Z., McNeilly, O., Ng, Y. H., Amal, R., Gunawan, C. (2021). Antibacterial activity of reduced graphene oxide. *Journal of Nanomaterials*, 2021(9941577), 1–10. <https://doi.org/10.1155/2021/9941577>
22. Meka Chufa, B., Abdisa Gonfa, B., Yohannes Anshebo, T., Adam Workneh, G. (2021). A novel and simplest green synthesis method of reduced graphene oxide using methanol extracted vernonia amygdalina: large-scale production. *Advances in Condensed Matter Physics*, 2021. <https://doi.org/10.1155/2021/6681710>
23. Mombeshora, E. T., Muchuweni, E. (2023). Dynamics of reduced graphene oxide: synthesis and structural models. *RSC Advances*, 13(26), 17633–17655. <https://doi.org/10.1039/d3ra02098c>
24. Mulia, D. S., Rahayu, S. D., Suyadi, A., Mujahid, I., Isnansetyo, A. (2023). Antibacterial activity of mangrove plant extract of *Rhizophora apiculata* in inhibiting the growth of various strains of *Aeromonas hydrophila*. *Biodiversitas*, 24(9), 4803–4810. <https://doi.org/10.13057/biodiv/d240921>
25. Nandiyanto, A. B. D., Oktiani, R., Ragadita, R. (2019). How to read and interpret FTIR spectroscopy of organic material. *Indonesian Journal of Science & Technology*, 4(1), 97–118. <https://doi.org/10.17509/ijost.v4i1.15806>
26. Nawaz, M. H., Iqbal, N., Rehman, R., Lim, J. W., Shahid, M. K. (2017). Green Synthesis and Characterization of Reduced Graphene Oxide. In *International Conference on “Applied Nanotechnology and Nanoscience” (ICANN 2017)*, 29–34. <https://doi.org/10.32434/0321-4095-2023-149-4-69-76>
27. Panicker, N. J., Sahu, P. P. (2021). Green reduction of graphene oxide using phytochemicals extracted from Pomelo Grandis and Tamarindus indica and its supercapacitor applications. *Journal of Materials Science: Materials in Electronics*, 32, 15265–15278. <https://doi.org/10.1007/s10854-021-06077-0>
28. Parthipan, P., Al-dosary, M. A., Al-ghamdi, A. A., Subramania, A. (2021). Eco-friendly synthesis of reduced graphene oxide as sustainable photocatalyst for removal of hazardous organic dyes. *Journal of King Saud University - Science*, 33(101438), 1–9. <https://doi.org/10.1016/j.jksus.2021.101438>
29. Parthipan, P., Cheng, L., Rajasekar, A., Govarthanan, M., Subramania, A. (2021). Biologically reduced graphene oxide as a green and easily available photocatalyst for degradation of organic dyes. *Environmental Research Journal*, 196(110983), 1–10.
30. Perumal, D., Albert, E. L., Saad, N., Hin, T. Y. Y., Zawawi, R. M., Teh, H. F., Che Abdullah, C. A. (2022). Fabrication and Characterization of *Clina-canthus nutans* Mediated Reduced Graphene Oxide Using a Green Approach. *Crystals*, 12(1539), 1–16. <https://doi.org/10.3390/cryst1211539>
31. Phukan, P., Narzary, R., Sahu, P. P. (2019). A green approach to fast synthesis of reduced graphene oxide using alcohol for tuning semiconductor property. *Materials Science in Semiconductor Processing*, 104(June), 104670. <https://doi.org/10.1016/j.mssp.2019.104670>
32. Punniyakotti, P., Aruliah, R., Angaiah, S. (2021). Facile synthesis of reduced graphene oxide using *Acalypha indica* and *Raphanus sativus* extracts and their in vitro cytotoxicity activity against human breast (MCF - 7) and lung (A549) cancer cell lines. *3 Biotech*, 11(157), 1–11. <https://doi.org/10.1007/s13205-021-02689-9>
33. Qi, J., Zhang, S., Xie, C., Liu, Q., Yang, S. (2021). Fabrication of *Erythrina senegalensis* leaf extract mediated reduced graphene oxide for cardiac repair applications in the nursing care. *Inorganic and Nano-Metal Chemistry*, 51, 1–7. <https://doi.org/10.1080/24701556.2020.1769663>
34. Rai, S., Bhujel, R., Biswas, J., Swain, B. P. (2020). Biocompatible synthesis of rGO from ginger extract as a green reducing agent and its supercapacitor application. *Bulletin of Materials Science*, 44(40), 1–11. <https://doi.org/10.1007/s12034-020-02318-w>
35. Rajab, A., Wahab, A. W., Taba, P., Kasim, S., Arif, A. R., Fatimah, Yasser, M. (2025). Methanolic leaf extract of *Indigofera tinctoria* mediated biosynthesis of zinc oxide nanoparticles. *Ecological Engineering and Environmental Technology*, 26(4), 300–310. <https://doi.org/10.12912/27197050/201328>
36. Rajan, R., Srinivasan, S., Wankhar, W., Rathinasamy, S. (2015). GC-MS analysis of indigofera tinctoria and its protective effect on noise induced behavioral and biochemical alterations in rats. *Research & Reviews: Journal of Pharmaceutical Analysis*, 4(2), 72–83.
37. Rakkimuthu, R., Aarthi, S., Neelamathi, E., Sathishkumar, P., Anandakumar, A. M., Sowmiya, D. (2022). Green synthesis of reduced graphene oxide silver nanocomposite using *Anisomeles Malabarica* (L.) R. Br. Leaf extract and its antibacterial activity. *Rasayan Journal of Chemistry*, 15(1), 417–422. <https://doi.org/10.31788/RJC.2022.1516786>
38. Sabayan, B., Goudarzian, N., Moslemin, M. H., Mohebat, R. (2020a). Green synthesis and high efficacy method for reduced graphene oxide by zataria multiflora extract. *Journal of Environmental Treatment Techniques*, 8(1), 488–496.
39. Sabayan, B., Goudarzian, N., Moslemin, M. H., Mohebat, R. (2020b). Green synthesis and high efficacy method for reduced graphene oxide by zataria multiflora extract. *Journal of Environmental Treatment Techniques*, 8(1), 488–496.
40. Sabee, M. M. S., Awang, M. S., Bustami, Y., Hamid, Z. A. (2020). Gentamicin loaded PLA microspheres

- susceptibility against *Staphylococcus aureus* and *Escherichia coli* by Kirby-Bauer and micro-dilution methods. In *AIP Conference Proceedings* (Vol. 2267). AIP Publishing.
41. Shahane, S., Sidhaye, D. (2018). Facile biosynthesis of reduced graphene oxide nanostructures via reduction by *tagetes erecta* (marigold flower) plant extract. *International Journal of Modern Physics B*, 32(1840068), 1–5. <https://doi.org/10.1142/S0217979218400684>
 42. Shubha, P., Namratha, K., Aparna, H. S., Ashok, N. R., Mustak, M. S., Chatterjee, J., Byrappa, K. (2017). Facile green reduction of graphene oxide using *Ocimum sanctum* hydroalcoholic extract and evaluation of its cellular toxicity. *Materials Chemistry and Physics*, 198, 66–72. <https://doi.org/10.1016/j.matchemphys.2017.05.062>
 43. Singh, J., Jindal, N., Kumar, V., Singh, K. (2023). Role of green chemistry in synthesis and modification of graphene oxide and its application: A review study. *Chemical Physics Impact*, 6(March), 100185. <https://doi.org/10.1016/j.chphi.2023.100185>
 44. Tahir, A., Liaqat, F., Saleem, M., Shaik, M. R., Adil, S. F., Siddiqui, M. R. H., Khan, M. (2023). Eco-friendly synthesis of anti-microbial and anti-fungal binary metal oxide decorated reduced graphene oxide nanocomposites with complimenting density functional studies. *Journal of Saudi Chemical Society*, 27(5), 1–16. <https://doi.org/10.1016/j.jscs.2023.101710>
 45. Thiyagarajulu, N., Arumugam, S. (2021). Green synthesis of reduced graphene oxide nanosheets using leaf extract of *lantana camara* and its in-vitro biological activities. *Journal of Cluster Science*, 32(3), 559–568. <https://doi.org/10.1007/s10876-020-01814-7>
 46. Venkatachalam, D. (2018). Pharmacognostic investigations and preliminary phytochemical studies of *Indigofera tinctoria* Linn. *International Journal of Pharmacognosy*, 5(11), 732–737. [https://doi.org/10.13040/IJPSR.0975-8232.IJP.5\(11\).732-37](https://doi.org/10.13040/IJPSR.0975-8232.IJP.5(11).732-37)
 47. Vijayan, R., Joseph, S., Mathew, B. (2018). *Indigofera tinctoria* leaf extract mediated green synthesis of silver and gold nanoparticles and assessment of their anticancer, antimicrobial, antioxidant and catalytic properties. *Artificial Cells, Nanomedicine and Biotechnology*, 46(4), 861–871. <https://doi.org/10.1080/21691401.2017.1345930>
 48. Wahyuningsih, S., Ramelan, A. H., Wardani, D. K., Aini, F. N., Sari, P. L., Tamtama, B. P. N., & Kristiawan, Y. R. (2017). Indigo Dye Derived from *Indigofera tinctoria* as Natural Food Colorant. In *IOP Conference Series: Materials Science and Engineering* 193, 1–5. <https://doi.org/10.1088/1757-899X/193/1/012048>
 49. Wijaya, R., Andersan, G., Per, S., Irawaty, W. (2020). Green reduction of graphene oxide using kaffir lime peel extract (*citrus hystrix*) and its application as adsorbent for methylene blue. *Scientific Re*, 10, 1–9. <https://doi.org/10.1038/s41598-020-57433-9>
 50. Yang, J., Xia, X., He, K., Zhang, M., Qin, S., Luo, M., Wu, L. (2021). Green synthesis of reduced graphene oxide (RGO) using the plant extract of *Salvia spinosa* and evaluation of photothermal effect on pancreatic cancer cells. *Journal of Molecular Structure*, 1245, 131064. <https://doi.org/10.1016/j.molstruc.2021.131064>
 51. Yasser, M., A Asfar, A. M., Widiyanti, S. E. (2021). Antioxidants activities of secondary metabolite compounds from buni fruit (*Antidesma bunius* L.) seed extract. *Rasayan Journal of Chemistry*, 14(2), 1351–1355. <https://doi.org/10.31788/rjc.2021.1426288>
 52. Yasser, M., Badai, M., Thahir, R., Sukasri, A., Kurniawan. (2021). Antioxidant extraction from purple sweet potato (*Ipomea batatas* l.) using ultrasound assisted extraction (UAE). *Journal of Physics: Conference Series*, 2049(1). <https://doi.org/10.1088/1742-6596/2049/1/012027>
 53. Yasser, M., Rafi, M., Wahyuni, W. T., Asfar, A. M. I. A., Widiyanti, S. E. (2020). Total phenolic content of methanol extract from buni fruits (*Antidesma bunius* L.) water. *Journal of Physics: Conference Series*, 1655(1), 1–6. <https://doi.org/10.1088/1742-6596/1655/1/012029>
 54. Yasser, M., Rafi, M., Wahyuni, W. T., Widiyanti, S. E., Asfar, A. M. I. A. (2020). Total phenolic content and antioxidant activities of buni fruit (*Antidesma bunius* L.) in moncongloe maros district extracted using ultrasound-assisted extraction. *Rasayan Journal of Chemistry*, 13(1), 684–689. <https://doi.org/10.31788/RJC.2020.1315584>